Available online at www.sciencedirect.com
ScienceDirect
Physics Letters A 365 (2007) 489–494
PHYSICS LETTERS A
www.elsevier.com/locate/pla

Coupling effect on the electronic transport through dimolecular junctions

Meng-Qiu Long [a], Lingling Wang [a], Ke-Qiu Chen [a,*], Xiao-Fei Li [a], B.S. Zou [a], Z. Shuai [b]

[a] *Department of Applied Physics, Hunan University, Changsha 410082, China*
[b] *Key Laboratory of Organic Solids, Institute of Chemistry, Chinese Academy of Sciences, Beijing 100080, China*

Received 13 January 2007; accepted 1 February 2007

Available online 14 February 2007

Communicated by V.M. Agranovich

Abstract

Using nonequilibrium Green's function and first-principle calculations, we investigate the transport behaviors of a dimolecule device with two 1,4-Dithiolbenzenes (DTB) sandwiched between two gold electrodes. The results show that the intermolecular coupling effect plays an important role in the conducting behavior of the system. By changing the dihedral angles between the two DTB molecules, namely changing the magnitude of the intermolecular interaction, a different transport behavior can be observed in the system.

PACS: 85.65.+h; 73.63.-b; 32.15.Ar

1. Introduction

During the past decade, there is increasing interest in electronic transport properties through single molecules connected to two metallic electrodes because of many novel physical properties such as single-electron characteristics [1], negative differential resistance [2–4], electrostatic current switching [5–7] have been founded in such devices. Experimentally, many techniques, such as the mechanically controllable break junction [8], scanning tunneling microscope [9], atomic force microscope [10], and crossed wire tunneling junction method [11], have been developed to explore current–voltage characteristics. A number of different theoretical approaches [12–23] have also been used to describe electron transport processes in molecular devices. Various kinds of single-molecule junctions or molecular monolayer junctions, such as short organic molecule wires [24–33], long-chain polymers [34,35], fullerenes [36,37] and carbon nanotubes [38,39], and so on, have been reported. Especially, 1,4-Dithiolbenzene (DTB) is one of the systems most intensely studied since the self-assembled monolayer (SAM) measurement for the device with DTB was reported [8]. However, the theoretical results do not agree with the experimental results of Reed et al. well. The theoretical researchers have suggested many plausible origins of the discrepancy between calculations and the experiment, many situations have been simulated, such as, the effects of various geometry contacts between the molecule and electrode [40–42], different electrode surface [43], anchor atoms [17,44] and the interaction of intermolecule [45], and so on.

Recently, the authors [46] considered a possible configuration for the SAM: two parallel benzenes sandwiched between semi-infinite gold electrodes. For each benzene, one of the ends of the molecule is chemically bonded to a gold surface through the thiol end group, and the other end physical adsorbed to a gold surface. The effect of the distance between two electrodes on the transport behavior of the molecular device was studied in detail. Here, we extend our previous work and investigate the effects of the relative angle on the transport properties by changing the dihedral angles between the two benezene rings. The calculated results show that intermolecular interaction depend on the dihedral angles between the two benezene rings, and plays an important role in electronic transport in such structure.

* Corresponding author.
E-mail addresses: llwang@hnu.cn (L. Wang), keqiuchen@hnu.cn (K.-Q. Chen).

0375-9601/$ – see front matter
doi:10.1016/j.physleta.2007.02.027

2. Model and computational method

Fig. 1(a) shows a schematic of molecular device with part of the electrodes: two benzenes sandwiched between semi-infinite gold electrodes. One contact between one molecule and the electrode is a strong chemical bond through the thiol end group, while a certain distance exists between the electrode and the other end of the molecule, where the strong S–H bond has not been cleaved. For the second molecule, the contact situation is just reversed. The thiol end group of the molecule is positioned in the FCC site of the Au (111) surface. In the present work, we consider the relative angles effects on transport properties by keeping one molecule fixed and twisting the other molecule with different dihedral angles related to the first molecule. Fig. 1(b1)–(b6) describes the related positions of the two benzenes for several specials angles as $0, \pi/6, \pi/4, \pi/3, 5\pi/12$ and $\pi/2$, respectively.

In this Letter, the theoretical technique used to study the electrical properties of the molecular junction is the first-principles computational package, Transiesta-C, which is based on nonequilibrium Green's function (NEGF) combined with density functional theory (DFT), developed by Brandbyge and co-workers [19]. The method can treat the molecule–electrode system self-consistently under finite bias conditions. We first investigated the transmission coefficient, the projected density of state, and the molecular electronic state within the environment of the electrode under zero bias, and then illustrated the current–voltage behaviors for different relative angles between the two molecules. In the following calculations, the distance of the two electrodes is fixed as 10.5 Å.

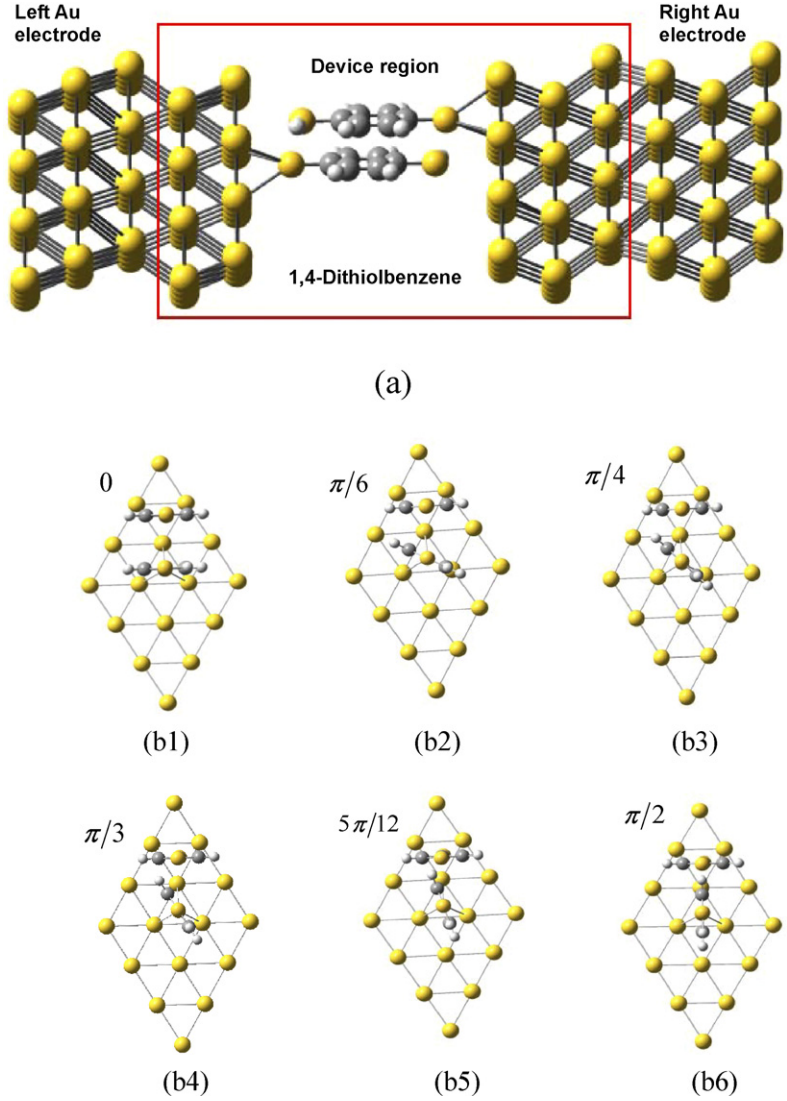

Fig. 1. (a) Schematic of the molecular device in our simulation. The gold electrodes form a (4×4) structure of the (111) surface, with 16 atoms in each layer. The (4×4) supercell is large enough to avoid any interaction with molecules in the next supercell. Left electrode contains 3 layers with the stacking (BCA), while the right electrode has the stacking (CBA). The stacking of the electrodes is chosen to match the central region which has the structure(BC-DTB-CBA). The complete two probe structure has the geometry, (BCA)BC-DTB-CBA(CBA). The periodical boundary conditions are applied in our system. (b1)–(b6) describe the related positions of the two benzenes by keeping one molecule fixed and twisting the other molecule with different dihedral angles 0, $\pi/6$, $\pi/4$, $\pi/3$, $5\pi/12$, and $\pi/2$, respectively.

3. Results and discussion

In Figs. 2 and 3, we plot the transmission coefficient $T(E)$ and partial density of states (PDOS) projected on the DTB bimolecular devices as a function of the electronic energy for different dihedral angles between the two thiolated benzenes at zero bias, respectively. The energy origin is set to be the Fermi level E_f of the system. It is clear seen from Figs. 2 and 3 that the $T(E)$ and the PDOS are strongly correlated, especially in the location of their peaks. The transmission curve consists of

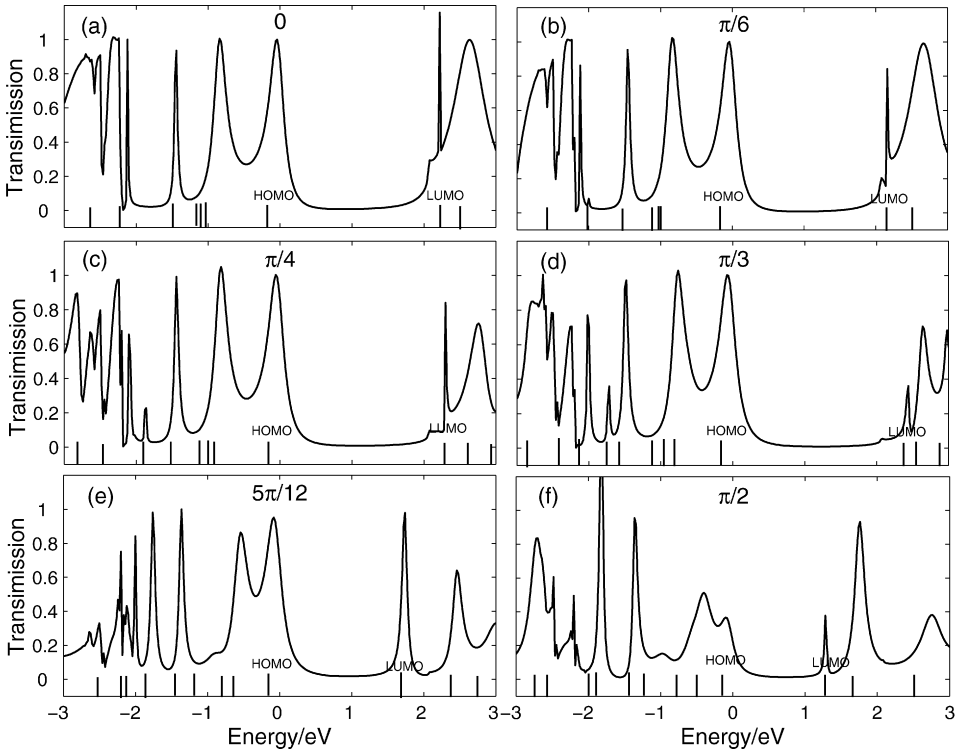

Fig. 2. Total transmission coefficient for the systems at zero bias voltage. The Fermi level E_f is chosen as the coordinate center. The vertical short lines represent the positions of the molecular orbital levels.

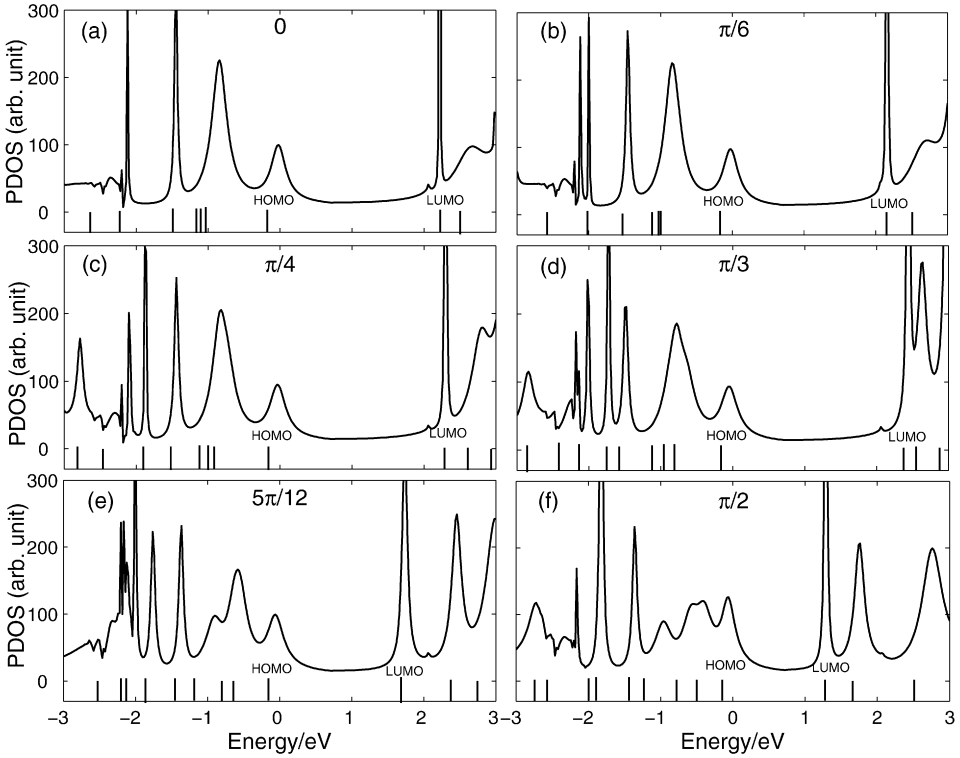

Fig. 3. The partial density of states (PDOS) projected in all systems at zero bias. The vertical short lines represent the positions of the molecular orbital levels.

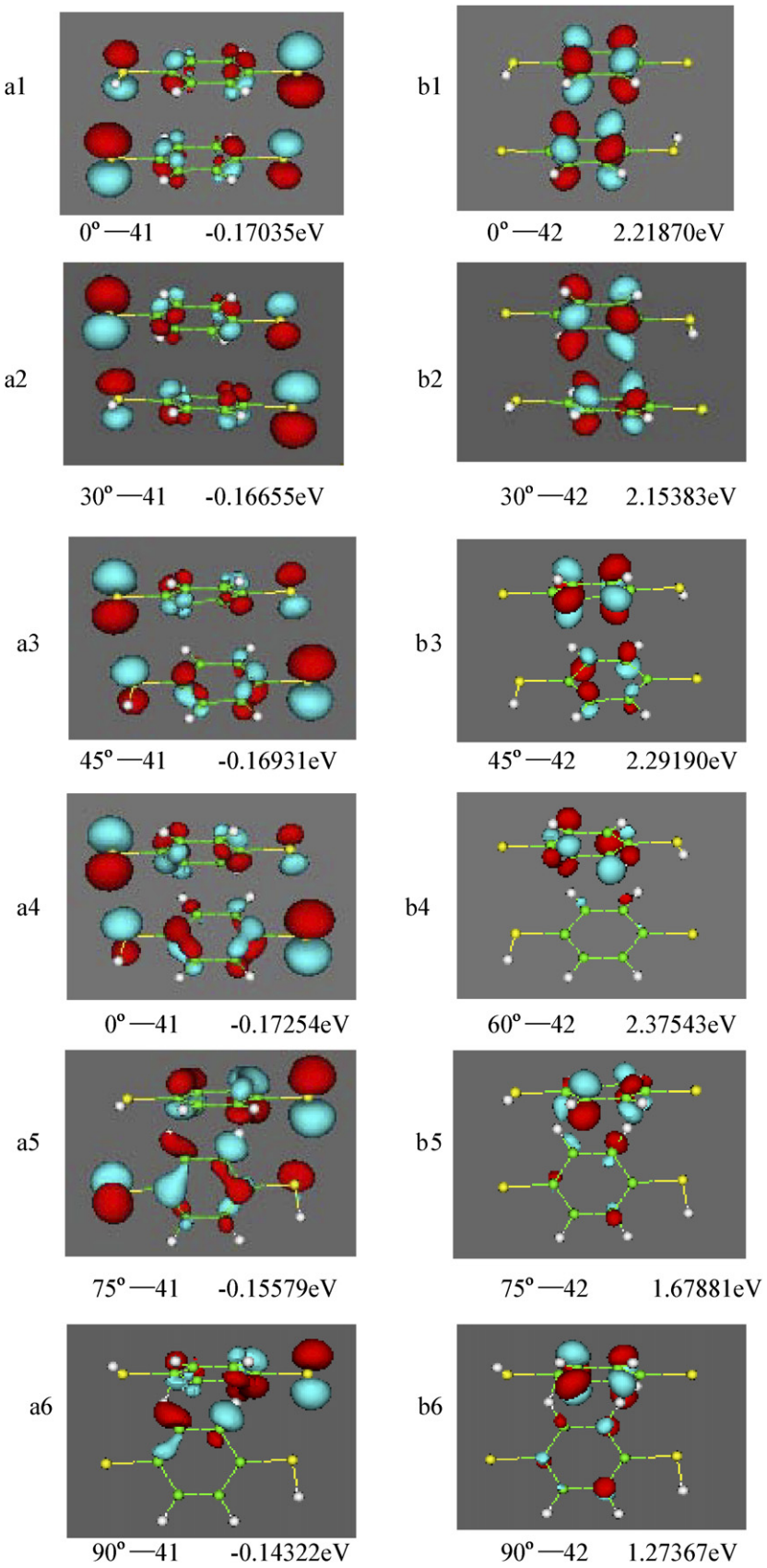

Fig. 4. Frontier orbitals of the MPSH. Figs. (a1)–(a6) are for the HOMO with the dihedral angles being 0, $\pi/6$, $\pi/4$, $\pi/3$, $5\pi/12$, and $\pi/2$, respectively. Figs. (b1)–(b6) are for the LUMO.

a series of valleys and peaks, and shows the same qualitative features as those of the projected PDOS. It is well known that the PDOS represents the discrete energy levels of the isolate molecule including the effects of energy shift and line broadening due to the molecule–electrode coupling. The transmission is determined by the electronic structure of the molecule and the coupling: the peak corresponds to the resonant transmission through the molecular states. From Fig. 2, we can see that the transmission coefficients are mainly characterized with a broadened feature due to the coupling between the molecule and gold electrodes. The highest occupied molecular orbital (HOMO) located at the first peak below E_f and approaches E_f, while the lowest unoccupied molecular orbital (LUMO), which is located at the first peak above E_f and far away from E_f. This means that at low bias the transmission is mainly dominated by the HOMO. By comparing Figs. 2(a)–(e), with (f), we find that the number of peaks are almost same for all cases, but the peak values, width of peaks, and their positions are different for different dihedral angles between the two thiolated benzenes. When the relative angles are small (as show in Figs. 2(a)–(d)), the difference is small. However when the angle is large enough (as show in Figs. 2(e)–(f)), we can find that two peaks appear near the LUMO, and the peaks near HOMO become smaller but broader. We also find that with the increase of the dihedral angles the positions of the peaks near LUMO shift towards E_f. These results indicate that when the dihedral angles between the two thiolated benzenes is smaller than $\pi/4$, its influence on the transmission is small. However it is increased further, the dihedral angles plays more and more role on the transmission spectra.

In order to understand the origins of the peaks in transmission coefficient, in Fig. 4, we plot the frontier orbitals of the molecular projected self-consistent Hamiltonian (MPSH), which is the self-consistent Hamiltonian of the isolated molecule in the presence of the Au electrode, namely, the molecular part extracted from the whole self-consistent Hamiltonian for the contact region. It contains the molecule–electrode coupling effects because during the self-consistent iteration, the electron density is for the contact region as a whole, however, the MPSH does not include the self-energy of the electrodes. The imaginary part of the self-energy broadens the transmission peaks, while the real part gives a rigid shift of the peak relative to the MPSH states. If an orbital is delocalized across the molecule, an electron that enters the molecule at the energy of the orbital has a high probability of reaching the other end, and thus there is a corresponding peak in the transmission probability $T(E)$. We know the isolated DTB bi-molecule have 82 valence electrons, thus orbital 41 is the HOMO and orbital 42 is the LUMO. We can find that when the dihedral angles between the two benzenes is smaller than $\pi/3$, the HOMO orbitals almost delocalize the whole dimolecule, and have a high density on the sulfur atom, which means much stronger molecule–electrode interaction (see Figs. 4(a1)–(a5)). However, when the dihedral angles between the two benzenes is equal to $\pi/2$, the localized behavior occurs for the HOMO orbital (see Fig. 4(a6)). From Figs. 2(b1)–(b6), it can be found that the LUMO orbitals localized the center of the molecule mainly for all dihedral angles.

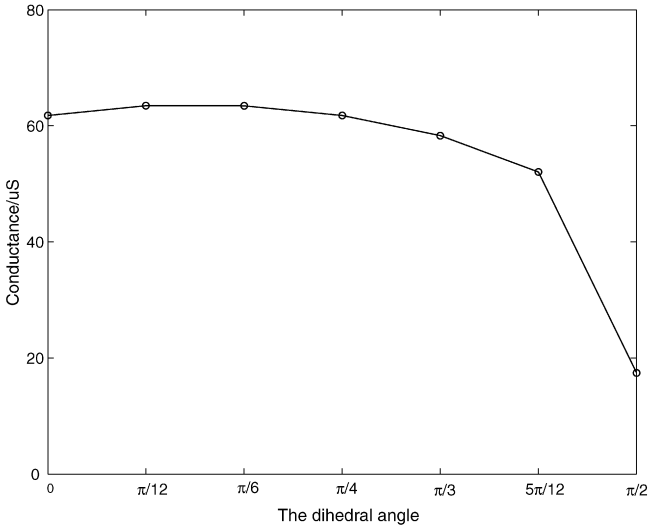

Fig. 5. The conductance as a function of the dihedral angels between the molecules.

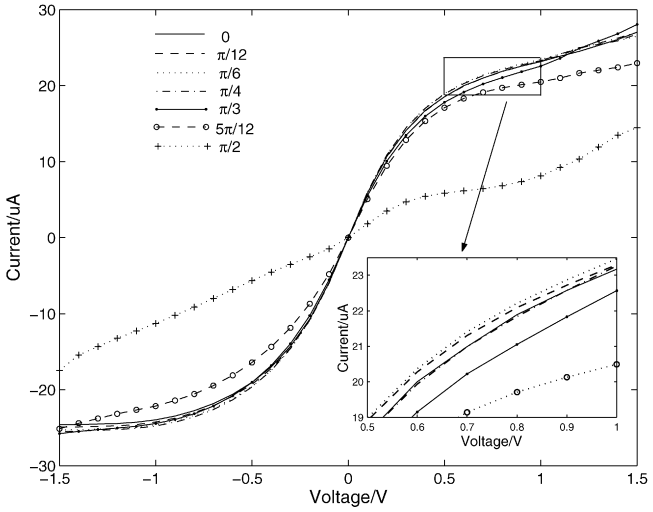

Fig. 6. The I–V curves of the bimolecular junctions for different dihedral angles between the molecules.

These results suggest that the transport behavior is mainly determined by the HOMO orbital at small bias.

In Fig. 5 we give the differential conductance at zero bias for different dihedral angle between the two benzene rings. It is found that when the dihedral angle twisted from 0 to $\pi/6$, the conductance increase slightly, and there is a maximum when the dihedral angle is about $\pi/6$. With further increasing the dihedral angle, the conductance decrease quickly. When the dihedral angle is equal to $\pi/2$, namely the two DTB molecules is perpendicular to each other, the differential conductance is of minimum. This can be understood from the fact that the MPSH orbital of HOMO is not delocalized across the whole molecule but localized at the center of the inter-molecule, as show in Fig. 4(a6). As a result, there is a small conductance for such a structure.

Fig. 6 describes the current–voltage (I–V) characteristics for different dihedral angles between the two benzene rings. Firstly, note that the current–voltage curves are asymmetrical

when the dihedral angle is not equal to zero. This is attributed to the fact that the systems is asymmetrical when the dihedral angel exists. From the figure, we can see clear that when the relative angles are smaller than $\pi/3$, the I–V curves are of small differences for different rotation angles especially for small bias. With the increasing of the dihedral angles, the current is decreased obviously. When dihedral angle is $\pi/2$ the current reaches the minimum. These results can be understood. From Fig. 4, it is known that the overlap between two molecules is obvious. It is the strong coupling between the two molecules that lead to the localization of electron in the molecules. As a result, the conductance and current are decreased obviously.

4. Summary

As a summary, the effect of the dihedral angles between the two molecules on the electron transport have been numerically simulated using the DFT-NEGF first principles method. The electron transmission coefficients, partial density of states, and I–V characteristics are calculated and analyzed for the systems with different dihedral angles. The results show that the dihedral angles play a critical role in determining the electron transmission in bimolecular device. The result will be helpful in understanding further the real situation in the molecular electronic device.

Acknowledgements

This work was supported by the National Natural Science Foundation of China (Nos. 90403026 and 10674044), and by Hunan Provincial Natural Science Foundation of China (No. 06JJ20004).

References

[1] R.P. Andres, T. Bein, M. Dorogi, S. Feng, J.I. Henderson, C.P. Kubiak, W. Mahoney, R.G. Osifchin, R. Reifenberger, Science 272 (1996) 1323.
[2] J. Chen, M.A. Reed, A.M. Rawlett, J.M. Tour, Science 286 (1999) 1550.
[3] J. Chen, W. Wang, M.A. Reed, A.M. Rawlett, D.W. Orice, J.M. Tour, Appl. Phys. Lett. 77 (2000) 1224.
[4] Y. Karzazi, J. Cornil, J.L. Bredas, J. Am. Chem. Soc. 123 (2001) 10076.
[5] C.P. Collier, E.W. Wong, M. Belohradsky, F.M. Raymo, J.F. Stoddart, P.J. Kuekes, R.S. Williams, J.R. Heath, Science 285 (1999) 391.
[6] D.I. Gittins, D. Bethell, D.J. Schiffrin, R.J. Nichols, Nature 408 (2000) 67.
[7] Z.J. Donhauser, B.A. Mantooth, K.F. Kelly, L.A. Bumm, J.D. Monnell, J.J. Stapleton, D.W. Price Jr., A.M. Rawlett, D.L. Allara, J.M. Tour, P.S. Weiss, Science 292 (2001) 2303.
[8] M.A. Reed, C. Zhou, C.J. Muller, T.P. Burgin, J.M. Tour, Science 278 (1997) 252.
[9] B.Q. Xu, N.J. Tao, Science 301 (2003) 1221.
[10] X.D. Cui, A. Primak, X. Zarate, J. Tomfohr, O.T. Sankey, A.L. Moore, T.A. Moore, D. Gust, G. Harris, S.M. Lindsay, Science 294 (2001) 571.
[11] J.G. Kushmerick, J. Naciri, J.C. Yang, R. Shashidhar, Nano Lett. 3 (2003) 897.
[12] V. Mujica, M. Kemp, M.A. Ratner, J. Chem. Phys. 101 (1994) 6849.
[13] N.D. Lang, Phys. Rev. B 52 (1995) 5335.
[14] M.P. Samanta, W. Tian, S. Datta, J.I. Henderson, C.P. Kubiak, Phys. Rev. B 53 (1996) R7626.
[15] M. Di Ventra, S.T. Pantelides, N.D. Lang, Phys. Rev. Lett. 84 (2000) 979.
[16] C.-K. Wang, Y. Fu, Y. Luo, Phys. Chem. Chem. Phys. 3 (2001) 5017.
[17] Y. Luo, C.-K. Wang, Y. Fu, J. Chem. Phys. 117 (2002) 10283.
[18] J. Taylor, H. Guo, J. Wang, Phys. Rev. B 63 (2001) 245407.
[19] M. Brandbyge, J.L. Mozos, P. Ordejon, J. Taylor, K. Stokbro, Phys. Rev. B 65 (2002) 165401.
[20] N.D. Lang, Ph. Avouris, Phys. Rev. B 64 (2001) 125323.
[21] Y. Xue, S. Datta, M.A. Ratner, Chem. Phys. 281 (2002) 151.
[22] Y. Xue, M.A. Ratner, Phys. Rev. B 68 (2003) 115407.
[23] S.-H. Ke, H.U. Baranger, W. Yang, Phys. Rev. B 70 (2004) 85410; J. Chem. Phys. 123 (2005) 114701.
[24] S.N. Yaliraki, M.A. Ratner, J. Chem. Phys. 109 (1998) 5036.
[25] S.N. Yaliraki, A.E. Roitberg, C. Gonzalez, V. Mujica, M.A. Ratner, J. Chem. Phys. 111 (1999) 6997.
[26] M. Di Ventra, S.T. Pantelides, N.D. Lang, Appl. Phys. Lett. 76 (2000) 3448.
[27] J. Reichert, R. Ochs, D. Beckmann, H.B. Weber, M. Mayor, H.V. Lohneysen, Phys. Rev. Lett. 88 (2002) 176804.
[28] Y. Luo, Y. Fu, J. Chem. Phys. 117 (2002) 10283.
[29] B. Xu, N.J. Tao, Science 301 (2003) 121.
[30] C.-K. Wang, Y. Luo, J. Chem. Phys. 119 (2003) 4923.
[31] K. Stokbro, J. Taylor, M. Brandbyge, J. Am. Chem. Soc. 125 (2003) 3674.
[32] S.-H. Ke, H.U. Baranger, W. Yang, J. Am. Chem. Soc. 126 (2004) 15897.
[33] P. Tarakeshwar, J.J. Palacios, D.M. Kim, J. Phys. Chem. B 110 (2006) 7456.
[34] W. Hu, H. Nakashima, K. Furukawa, Y. Kashimura, K. Ajito, K. Torimitsu, Appl. Phys. Lett. 85 (2004) 115.
[35] W. Hu, J. Jiang, H. Nakashima, Y. Luo, Y. Kashimura, K.-Q. Chen, Z. Shuai, K. Furukawa, W. Lu, Y. Liu, D. Zhu, K. Torimitsu, Phys. Rev. Lett. 96 (2006) 27801.
[36] H. Park, J. Park, A.K.L. Lim, E.H. Anderson, A.P. Alivisatos, P.L. Mceuen, Nature 407 (2000) 57.
[37] J. Taylor, H. Guo, J. Wang, Phys. Rev. B 63 (2001) 121104.
[38] S.J. Tans, A.R.M. Verschueren, C. Dekker, Nature 393 (1999) 49; Z. Yao, H.W.C. Postma, L. Balents, C. Dekker, Nature 402 (1999) 273.
[39] Z. Yao, H.W.C. Postma, L. Balents, C. Dekker, Nature 402 (1999) 273.
[40] S.-H. Ke, H.U. Baranger, W. Yang, J. Am. Chem. Soc. 126 (2004) 15897.
[41] H. Kondo, H. Kino, J. Nara, T. Ozaki, T. Ohno, Phys. Rev. B 73 (2006) 235323.
[42] A. Grigoriev, J. Sköldberg, G. Wendin, Ž. Crljen, Phys. Rev. B 74 (2006) 045401.
[43] H. Basch, R. Cohen, M.A. Ratner, Nano Lett. 5 (2005) 1668.
[44] P. Bai, E.L. Neerja, P. Collier, IEEE Trans. Nanotechn. 4 (2005) 1536.
[45] E.G. Emberly, G. Kirczenow, Phys. Rev. B 64 (2001) 235412.
[46] H. Geng, S. Yin, K.-Q. Chen, Z. Shuai, J. Phys. Chem. B 109 (2005) 12304.